JOURNAL OF MATERIALS SCIENCE 39 (2004) 1975–1985

Tailored microstructure of zirconia and hafnia-based thermal barrier coatings with low thermal conductivity and high hemispherical reflectance by EB-PVD

J. SINGH, D. E. WOLFE
Applied Research Laboratory, Penn State University, University Park, PA 16801, USA
E-mail: jxs46@psu.edu

R. A. MILLER, J. I. ELDRIDGE, DONG-MING ZHU
NASA-GRC, 21000 Brookpark Road, Cleveland, OH 44135, USA

Zirconia and hafnia based thermal barrier coating materials were produced by industrial prototype electron beam-physical vapor deposition (EB-PVD). Columnar microstructure of the thermal barrier coatings were modified with controlled microporosity and diffuse sub-interfaces resulting in lower thermal conductivity (20–30% depending up on microporosity volume fraction), higher thermal reflectance (15–20%) and more strain tolerance as compared with standard thermal barrier coatings (TBC). The novel processed coating systems were examined by various techniques including scanning electron microscopy (SEM), X-ray diffraction, thermal conductivity by laser technique, and hemispherical reflectance. © *2004 Kluwer Academic Publishers*

1. Introduction

The turbine industry is continuously making an effort to increase the thermal efficiency of the engine as well as the life of turbine components under severe environmental conditions including oxidation and corrosion at elevated temperatures. The life of turbine components is increased by applying oxidation-resistant coatings composed of platinum-aluminide (Pt-Al) or MCrAlY alloys (M = Ni, Co, Fe, or mixed combination) beneath a thermal barrier coating (TBC) composed of zirconia with 8 wt% yttria (8YSZ), which is an ideal candidate for thermal protection coatings because of its low density, low thermal conductivity, high melting point, good thermal shock resistance and excellent erosion resistant properties. 8YSZ has gained widespread acceptance as a TBC material for turbine applications and is generally applied by either the plasma spray or EB-PVD process [1]. TBC applied by EB-PVD process provide advantages over the plasma spray process that include better strain tolerance, erosion-resistance, bond strength, and surface roughness but with the disadvantage of having slightly higher initial thermal conductivity [1].

In thermally sprayed TBC, typical grain size is approximately 1–2 μm and the coating microstructure is associated with inter-splat boundary porosity, unmelted, partially melted particles and micro-cracks [2]. In EB-PVD, TBC grain sizes vary from 1 to 2 μm near the bond coating/TBC interface, while the TBC columnar grain length is often 100–250 μm in thickness with a high degree of crystallographic texture. Keeping the total thickness of the TBC constant, the alignment of the inter-splat boundaries (with typical spacing of 1 to 10 μm in the case of thermally sprayed coatings with voids, micro-cracks) has a more pronounced effect on thermal conductivity than with EB-PVD, reducing the thermal conductivity of zirconia-yttria TBC materials from the bulk theoretical values 2.2–2.6 W/mK to values in the range 0.7–0.9 W/mK. However, within the first few hours of turbine engine operation, the thermal conductivity of plasma sprayed TBC can increase to 1.5 W/mK due to high temperature sintering effect.

The inter-splat/microcracks/porosity provide initial low conductivity for the plasma sprayed coatings mainly because they are involved with air gaps—air is a good thermal insulator compared with zirconia (air has poor thermal conductivity), not because the reduced mean free path for photons/phonon. In addition, the splat boundaries are probably few compared to grain boundaries (1 micron or so grain size) in producing significant phonon scattering effect. Nevertheless, the inter-splat porosity and boundaries are more effective in reducing the thermal conductivity of the material than the columnar porosity in EB-PVD coatings because of the increased thermal resistance and phonon scattering in the heat conduction direction. If heat resistance and greater phonon scattering associated with the plasma sprayed TBC microstructure could be applied to TBC produced by EB-PVD, it could make a significant contribution to the reduction of the thermal conductivity. In addition, radiative heat transport becomes increasingly important at high temperatures, so producing a TBC

microstructure that also increases infrared (IR) photon scattering will help decrease heat transport through the TBC at high temperatures. Thus, a modified microstructure of the EB-PVD TBC appears to be very promising method in lowering the thermal conductivity of the coating. Very limited research has been conducted in this area which could significantly impact the turbine industry by producing TBC materials with lower thermal conductivity for high temperature applications. It is important to distinguish the effects of phonon scattering, which decreases thermal conductivity, and photon scattering which reduces radiative heat transport. Both scattering properties are influenced by the presence of interfaces including voids, micro-porosity and grain boundaries; however, phonon scattering is effected by smaller dimension features than IR photon scattering.

Efforts are underway at different laboratories in developing new TBC materials or alloying 8YSZ for low thermal conductivity. Alloying 8YSZ with ceramic oxides including CeO_2 or replacing Y_2O_3 by Sc_2O_3 including ZrO_2-20 wt%Y_2O_3, ZrO_2-25% CeO_2 and ZrO_2-22% CeO_2-7 wt%Y_2O_3 reported to offer lower thermal conductivity, but also poor erosion resistant properties [3, 4]. Similarly, the addition of rare-earth oxide dopants to ZrO_2 is reported to offer lower thermal conductivity i.e., additions of Gd_2O_3, Sm_2O_3 and Yb_2O_3 to either ZrO_2 or 8YSZ [5].

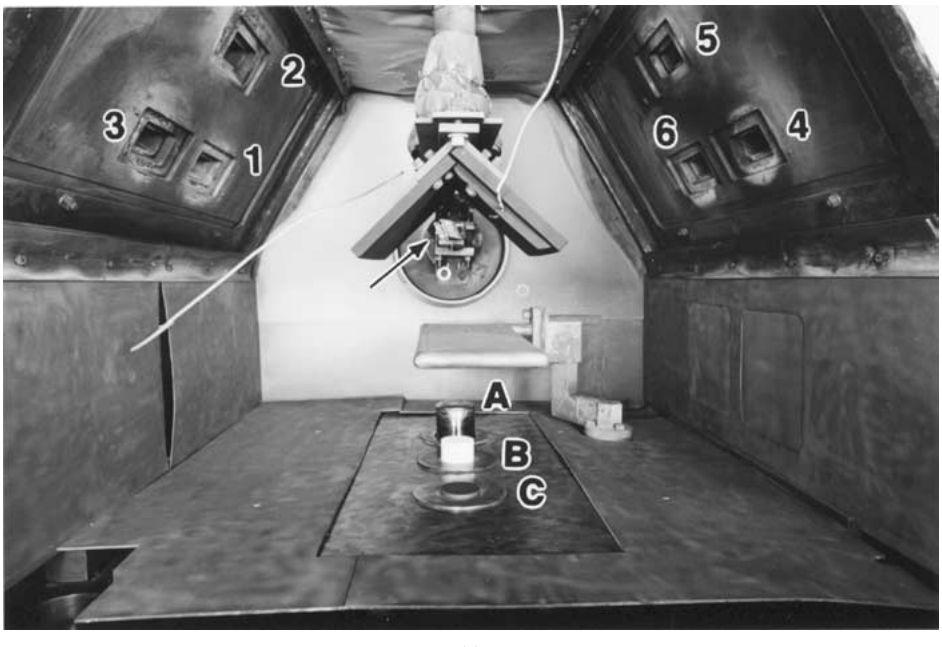

(a)

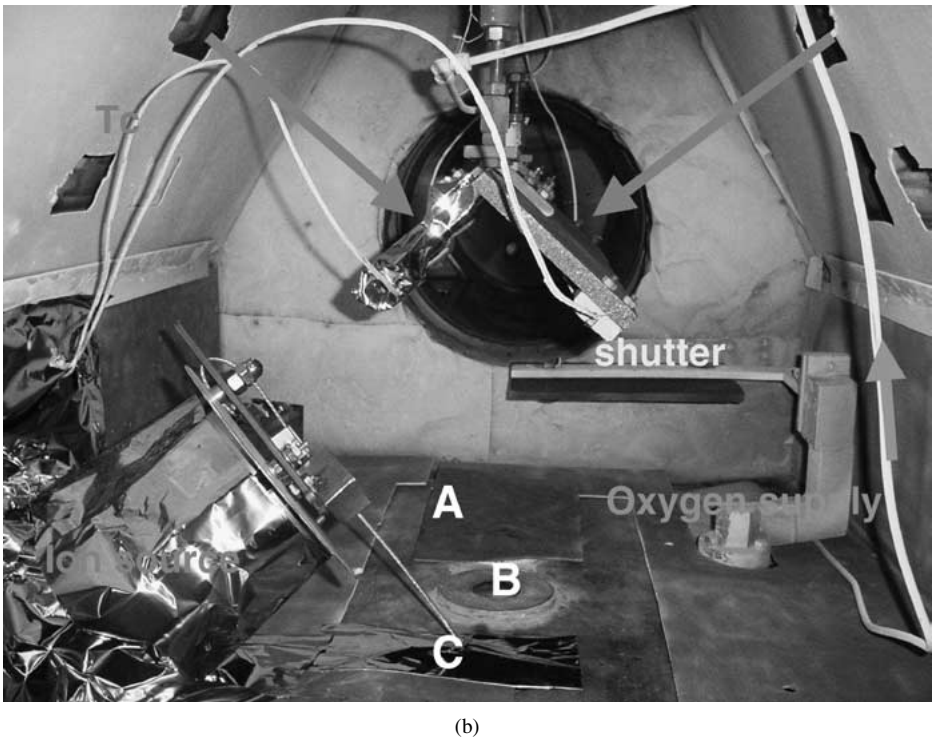

(b)

Figure 1 (a) Photograph of EB-PVD chamber. (b) Photograph of EB-PVD chamber with ion source.

The main objective of the present investigation was to modify the TBC microstructure with controlled, decorated micro-porosity during EB-PVD deposition process for reducing thermal conductivity without sacrificing other desirable properties previously discussed. In addition, thermal reflectance of the coatings can be enhanced by creating multiple interfaces. The advantage of this approach is that it can be applied to other TBC materials to further reduce their thermal conductivity. Combining both properties of low thermal conductivity and high reflectance should have a dramatic impact on the performance of turbine components including increasing the thrust-to-weight ratio, reducing fuel consumption by more than 1% and increasing component life.

2. Experimental procedure

Penn State University has a unique industrial prototype EB-PVD unit with six electron-beam guns, and 8″ diameter ion source (Fig. 1a and b). Four EB-guns can be used to evaporate the coating materials and two EB-guns can be used to preheat the substrate to facilitate coating adhesion. Each gun has an average power of 45 kW with a peak capacity of 65 kW for a total power of 270 kW. In addition, the chamber has a three-ingot continuous feeding system (A, B and C as shown in Fig. 1). Overall, the main deposition chamber size is approximately 90 cm in length, 90 cm in width, and 90 cm in height. The maximum substrate diameter with vertical rotation that can be accommodated is 40 cm. Parts can be manipulated in three dimensions on a computer-controlled rack system at a speed of 5.5 to 110 rpm and with a maximum load of approximately 100 kg. Physical vapor deposition (PVD) is primarily a line-of-sight process; therefore, uniform coatings of complex parts, such as turbine blades, are produced by continuously rotating the components during the coating process. Deposition rate and coating thickness depend on various variables including the material being deposited, deposition time, chamber pressure, electron beam operating power, and the source-to-substrate distance (i.e., the distance between the evaporant and components to be coated). The rotating components are often isolated from the incoming vapor flux at the start of the deposition process using a shutter until the melt pool is stabilized. During this investigation, test coupons were mounted on a horizontal 5.08 cm diameter stainless steel shaft which was rotating 30.5 cm above the melt pool at a speed of 7 revolutions per minute (rpm). During the ingot evaporation process, external oxygen was injected into the vapor cloud at a flow rate of 100–150 sccm in order to compensate for the loss of oxygen from the source material and to maintain the desired stochiometric TBC composition. Typical deposition chamber pressure was 1×10^{-3} Torr.

Pt-aluminide bond coated nickel-based super alloy Rene N-5 samples were used in the present investigation. The bond coated samples were ultrasonically cleaned in acetone for twenty minutes, followed by rinsing with de-ionized water and then cleaned with methyl alcohol for ten minutes. Samples were again rinsed with de-ionized water and then dried with nitrogen gas. The samples were then tack welded separately onto a 1×1 inch stainless steel foil and again cleaned using an ultrasonic bath cleaner in the above-mentioned solutions and mounted on a mandrel for TBC deposition. Fracture surfaces and surface morphology of the coated samples were examined by a scanning electron microscope (SEM). Phase analysis of the coated samples was determined by X-ray diffraction. Thermal conductivity of the TBC was measured by the steady state heat flux CO_2 laser technique at 1316°C and IR hemispherical reflectance was measured in an FTIR spectrometer with an integrating sphere accessory at room temperature [5, 6].

3. Results and discussion

3.1. ZrO_2–8% Y_2O_3

The typical microstructure of a TBC produced by EB-PVD can be divided into two zones (Fig. 2a). The inner zone (I) is the early part of multiple nucleation and subsequent growth of the columnar microstructure having large number of interfaces, grain boundaries, micro-porosity and randomly oriented grains. The thickness of the inner zone ranges from 5 to 10 μm and exhibits lower thermal conductivity (around 1.0 K/mK). With increasing thickness, the structure is characterized by a high-aspect ratio columnar grain with dominant crystallographic texture. The thermal conductivity increases as the outer part of the coating

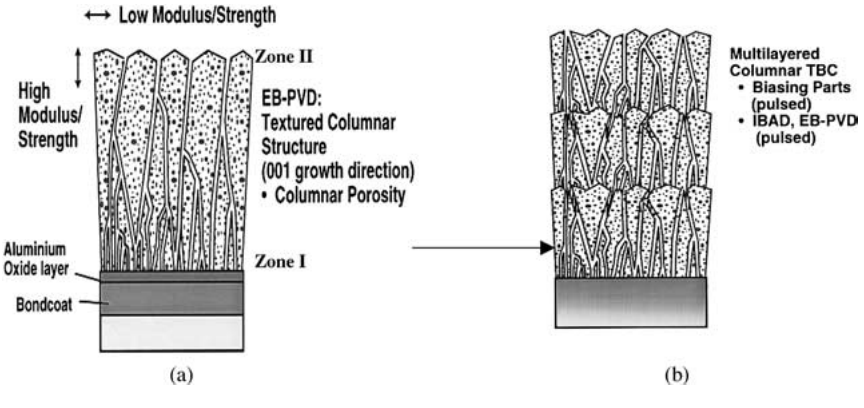

Figure 2 Schematic diagram showing (a) a typical standard vapor phase columnar microstructure and (b) modified columnar microstructure with multiple interfaces.

becomes more crystallograhically perfect (zone II). In this outer zone (II), the thermal conductivity approaches that of bulk zirconia (2.2 W/mK). Thus, modifying TBC structures should offer the best properties available for commercial EB-PVD coatings: namely, low thermal conductivity, high strain tolerance, and good erosion resistance. Combination of layering at the micron level and introduction of density changes from layer to layer will significantly reduce the thermal conductivity of the coating (Fig. 2b). As mentioned earlier, layered periodicity in the coating will significantly reduce both the phonon scattering and photon transport. The local changes in density resulting from "shuttering" the condensing vapor flux

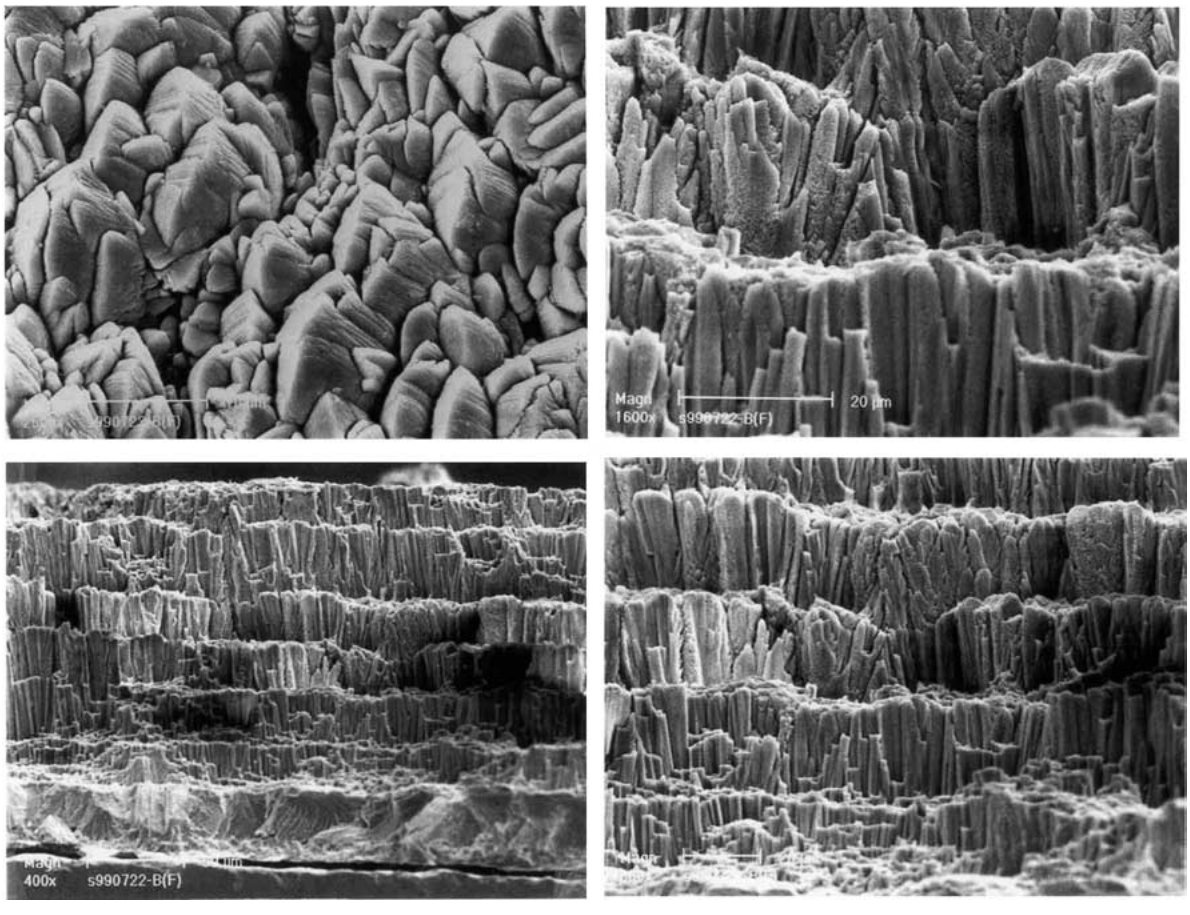

Figure 3 SEM micrographs showing a fracture surface of 8YSZ produced by EB-PVD using "in & out" method exhibiting multiple sharp interfaces.

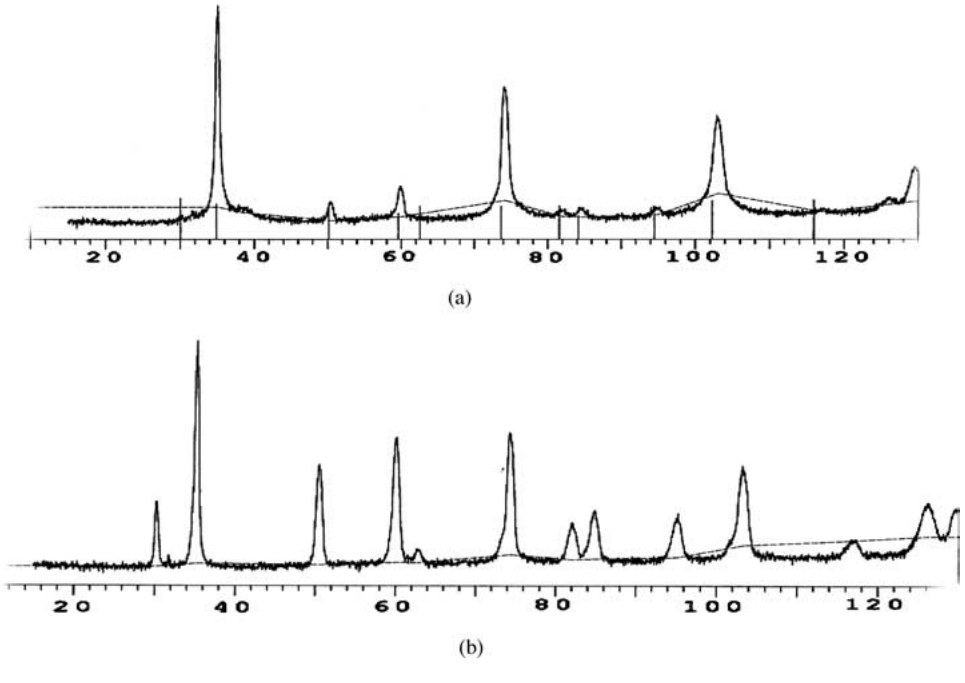

Figure 4 X-ray diffraction of TBC produced by in & out approach with 40 layers by EB-PVD: (a) standard TBC-single layer and (b) multiple interfaces.

contribute to phonon scattering and thus reduce the thermal conduction.

Microporosity in the TBC was incorporated by two approaches. The *first approach* used was to periodically interrupt the continuous vapor flux by translating the sample away from the vapor cloud for a short period (30–60 s) and then re-introduce the samples into the vapor cloud. During this interruption, the temperature of the sample decreased to approximately 700–800°C from 1000°C. Due to the combination of discontinuous condensation and thermal fluctuations of the sample's surface temperature during this "in and out" method, new grain formation occurs (similar concept as with inter-splat boundaries in plasma sprayed TBC). It was theorized that during nucleation and subsequent growth of the first TBC layer on the polycrystalline PtAl coated substrate, the TBC would exhibit more randomly oriented grains (i.e., similar to zone I of Fig. 2a, which generally occurs during standard single layer 8YSZ deposition). After the interruption, the subsequent nucleation of the second layer (on the previous grown textured layer (zone II)) will again exhibit crystallographic texturing similar to zone I resulting in more random texturing. As additional material deposits on the sample, the grains grow with the zone II structure and crystallographic texture. After each interruption, there will be sharp interface between the new grains and the previously formed grains as shown in Fig. 3a–c. Due to the faceted surface morphology of columnar grains, additional microporosity develops at or near each interface of the next nucleating TBC layer. The interfacial volume fraction of the distinct

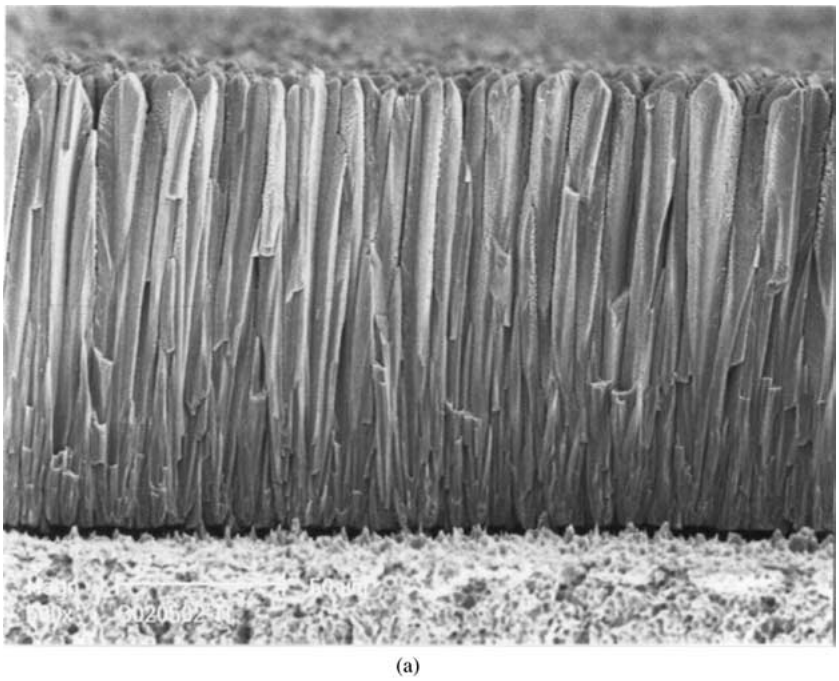

(a)

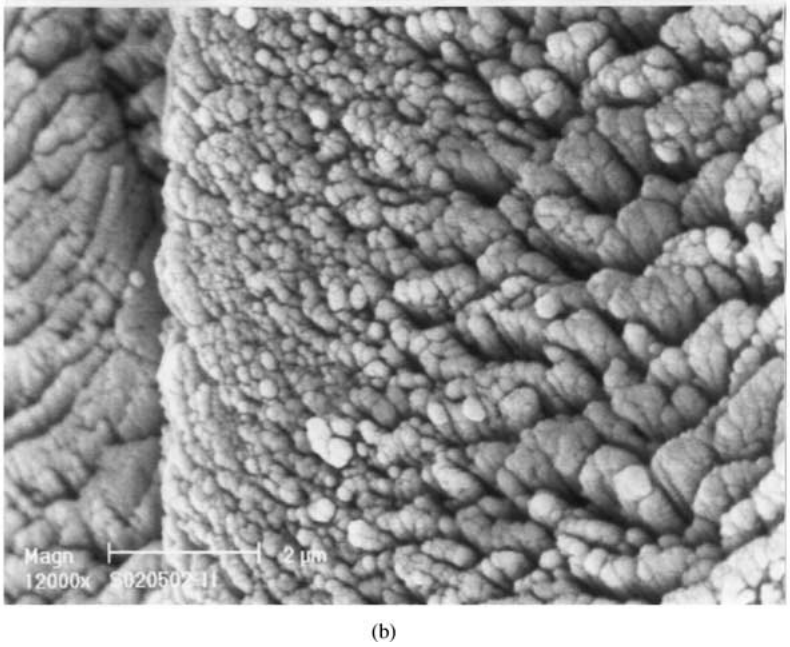

(b)

Figure 5 SEM micrographs showing a fracture surface of 8YSZ deposited by EB-PVD having 40-layers using the "shutter" method at (a) low and (b) high magnification.

interfaces and degree of microporosity depends on the periodicity or total number of layers. This concept is referred to as the "in & out" approach as shown in Fig. 2b and 3a–c. By increasing the total number of layers, the volume fraction of randomly oriented grains (near zone I of each layer) increases and as anticipated, was found to be less crystallographically textured when compared to a standard single-layered TBC. This was confirmed by X-ray diffraction patterns as shown in Fig. 4. In general, a standard single layered 8YSZ coating shows a strong (002) crystallographic texture. Although the layered TBC (Fig. 4b) shows a (002) crystallographic orientation, the observance of additional high index planes in the TBC could be due to many factors including high volume fraction of multiple nucleation and growth of grains [1]. The subsequent growth of these grains during deposition will change its crystallographic growth orientation, as discussed below. The change in grain orientation is believed to be the result of the competition between strain energy and surface free energy.

The *second approach* used was to periodically interrupt the continuous flux of the vapor cloud by using a "shutter" mechanism. It is important to mention here that the temperature of the substrate remained fairly constant during the deposition process (whereas it decreased to 700–800°C during the "in and out" method), but discontinuous vapor condensation still occurred. During this interruption period, it is believed that the surface mobility of the condensed species contribute towards the surface relaxation of the deposited coating. As the vapor flux is prevented from condensing on the surface, the surface atoms have enough time, energy and surface mobility to diffuse to regions of lower energy. As a result, the surface strains change resulting in more phonon scattering due to different strain energy fields and potentially sub-grains and interfaces, thus resulting in lower thermal conductivity. When the shutter is opened, the new flux deposits on a slightly different strained surface. This newly strained surface results in a very diffuse interface which may contain microporosity and intracolumnar morphology differences than that of a standard layered 8YSZ. By restricting the vapor flux from depositing on the surface, the initial atoms depositing on this newly strained surface start to condense in regions of lower energy until rapid condensation occurs which leads to island coalescence and again different strain energy fields. During this atom coalescence, stable microporosity and intracolumnar morphology differences develop with continued columnar growth. During the initial deposition, atoms form islands and grow until the flux rapidly increases resulting in grain coalescence producing microporosity. However, when viewed from the top surface, the grain size does not change, but the intracolumnar microstructure (i.e., microporosity and morphology) is believed to be altered as shown in Fig. 5a and b. Microporosity was not detected by SEM. Additional characterization is underway to confirm this analysis. Since there is no temperature change, and just a disruption of the vapor flux for a short period of time, the long high aspect ratio columnar grains continue to grow to the total length of the coating thickness similar to standard single layer 8YSZ. Comparison with a standard 8YSZ shows no distinct differences in macrostructure. Since the growth orientation of the new flux remains the same as the underlying grain, similar crystallographic texture occurs (Fig. 6), but can vary depending on the total number of "shuttered" layers. The interface between the condensed flux and the newly arrived flux is diffuse (i.e., no sharp distinct interface) which results in microporosity near the interface. Such microstructural modifications will have an impact on the thermal conductivity. This theory was confirmed by measuring the thermal conductivity and hemispherical reflectance of the layered TBC deposited by both approaches as discussed below.

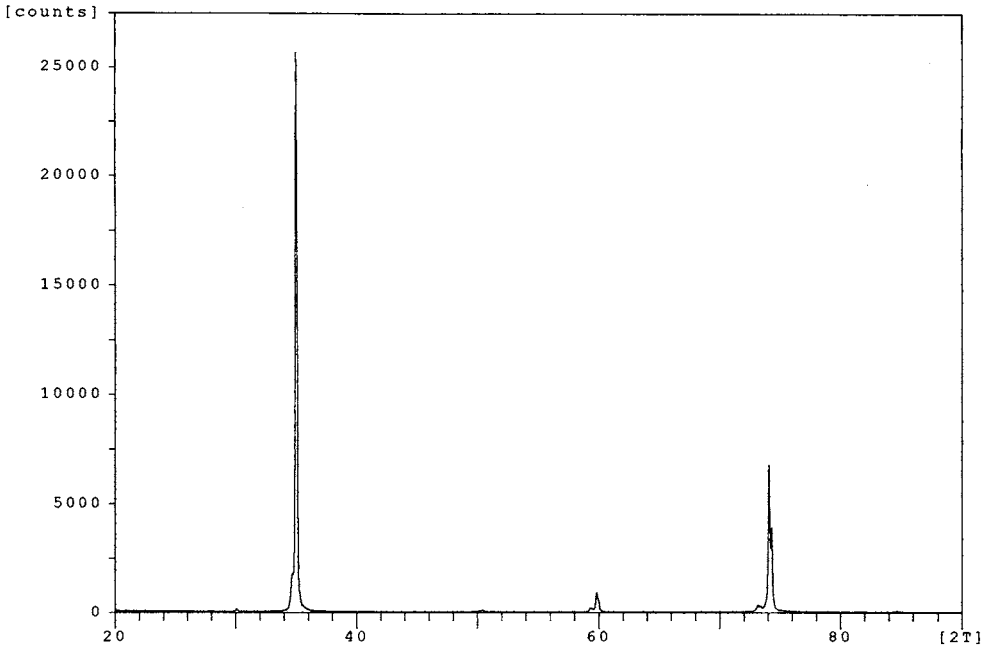

Figure 6 X-ray diffraction of TBC produced by shutter with 40 layers by EB-PVD showing texturing along ⟨200⟩.

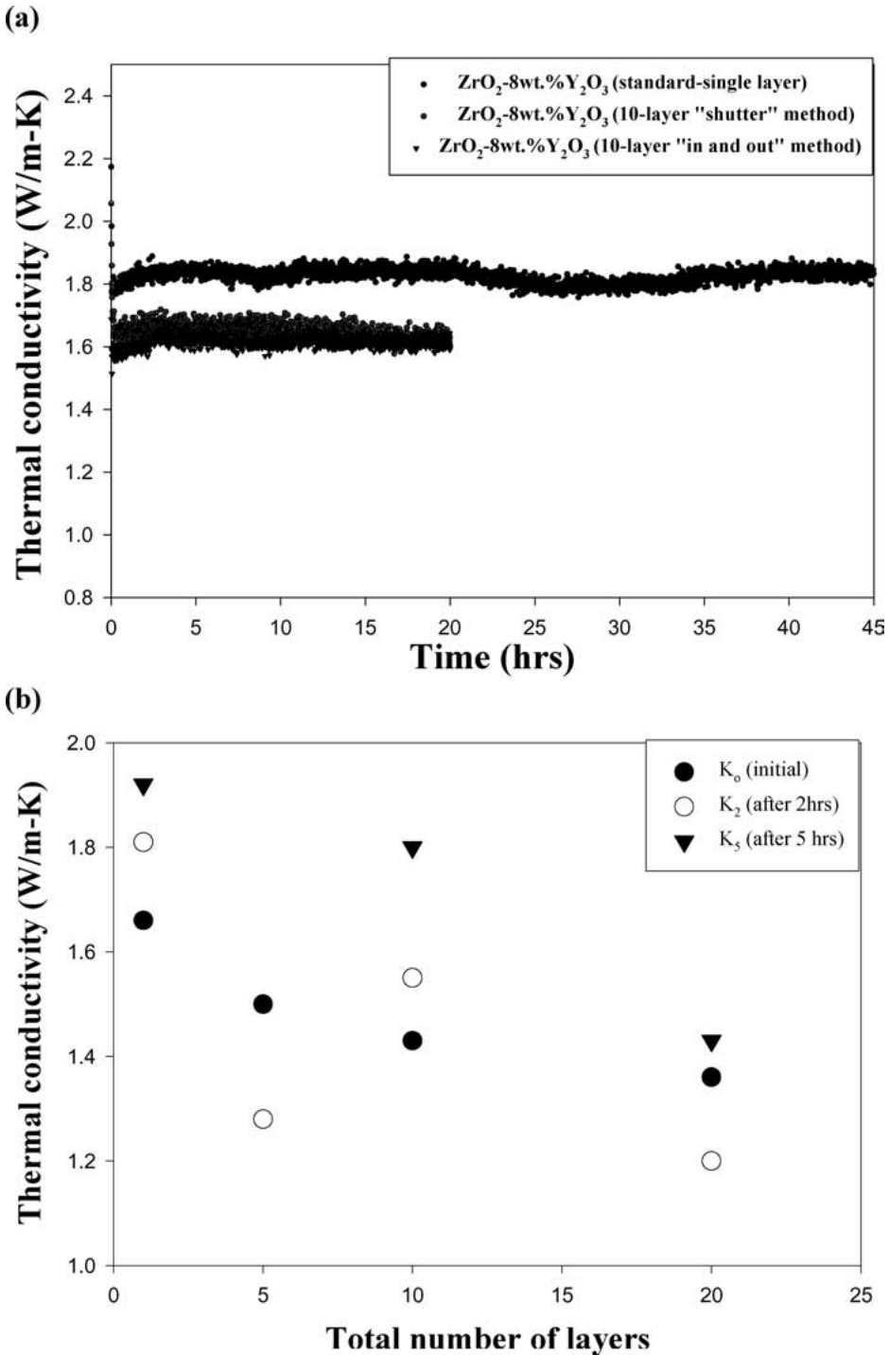

Figure 7 Thermal conductivity of EB-PVD 8YSZ coatings determined by a steady-state laser heat flux technique at 1316°C showing (a) Thermal conductivity of EB-PVD 8YSZ coatings produced by: standard continuous evaporation, interruption of the vapor flux by "shutter" and interruption of flux by "in and out" method, as a function of testing time. (b) Thermal conductivity of EB-PVD as a function of total number of layers produced by the "shutter" method, measure at various stages of testing, where k_0 = as deposited, k_2 = after 2 h, and k_5 after 5 h of testing.

Fig. 7a shows comparative thermal conductivity of a standard single layered 8YSZ, layered TBC with diffuse interface produced by "shutter" method, and layered TBC with sharp interface produced by "in & out" concept. The thermal conductivity of the 10-layered TBC (shutter) is comparable with the 10-layered TBC produced by "in & out". In order to establish a relationship between the thermal conductivity as a function of total number of TBC layers, additional TBC coated samples were produced using the shutter concept. It was established that the thermal conductivity decreased linearly as a function of increasing number of TBC layers as shown in Fig. 7b. This confirms the theory that periodic interruption of the incoming flux by "shutter" method results in lower thermal conductivity as compared to a standard 8YSZ.

In addition to decreasing thermal conductivity, the diffused interfaces with microporosity should also affect the hemispherical reflectance of the coating and therefore reduce radiative heat transport through the TBC. As shown in Fig. 8, the reflectance of the coating increases as function of total number of layers at 1 μm wavelength. The reflectance was increased from approximately 35% (1-layer) to 45% (20-layers) at 1 μm

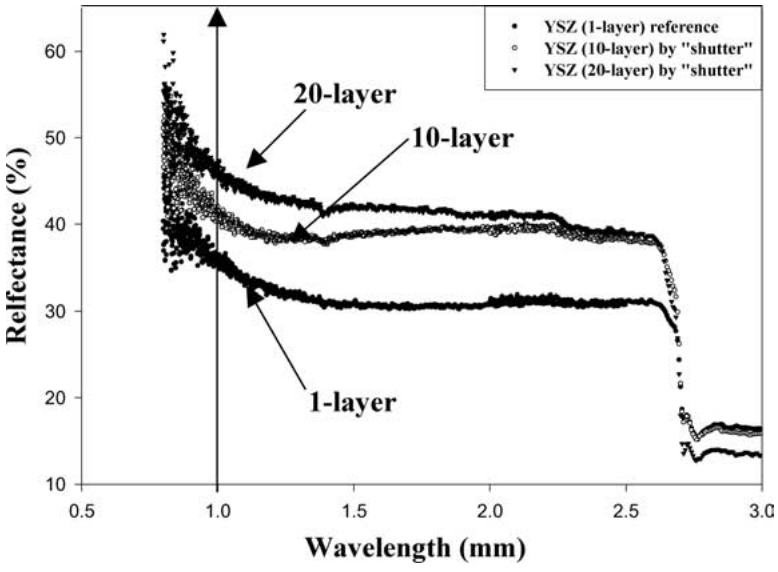

Figure 8 Hemi-spherical reflectance of layered (1, 5, 10, and 20 total layers) EB-PVD 8YSZ TBC deposited the "shutter" method after thermal exposure at 950°C for 20 h.

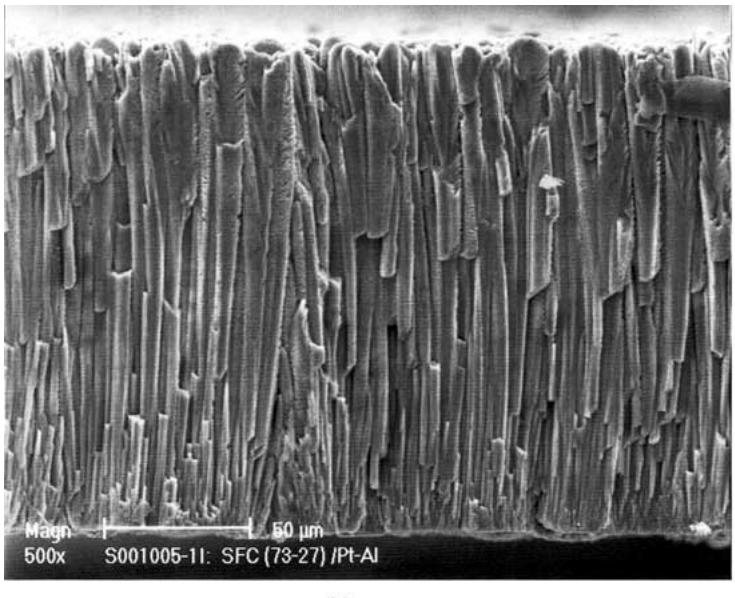

(a)

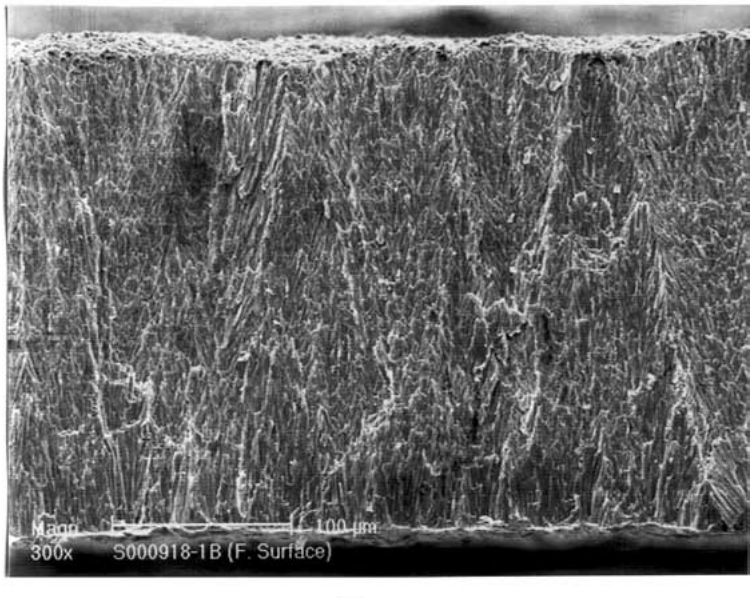

(b)

Figure 9 SEM micrographs showing a fracture surface of the growth morphology of (a) HfO_2-40 wt%ZrO_2-20 wt% Y_2O_3 and (b) HfO_2-27 wt%Y_2O_3 TBC materials deposited by EB-PVD at 1000°C.

wavelength. This suggests that more heat will be reflected from the coatings as the number of layers increases within the TBC. Reflectance of the layered TBC produced by "in & out" was increased from ~40 to 55% as the total number of sharp interfaces increased from 10 to 40 at 1 μm wavelength.

The layering concept has opened an opportunity in engineering TBC with desired higher reflectance and lower thermal conductive properties through microstructural modifications. The layering concept was extended to HfO_2-base alloyed ceramic coatings as well as engineering new TBC materials in exhibiting high reflectance properties over a wide wavelength range.

3.2. HfO_2-based ceramic coatings

The effort was undertaken to define the process window in applying HfO_2-40 wt%ZrO_2-20 wt%Y_2O_3 and HfO_2-27 wt%Y_2O_3 coatings on Pt-aluminide bond coated Rene N5 buttons. Coatings were applied using the standard process parameters used for 8YSZ, i.e., substrate temperature of 1000°C, external injected oxygen ~150 Sccm, rotation speed of 7 rpm, and 30.5 cm source-to-substrate distance. The HfO_2-40 wt% ZrO_2-20 wt%Y_2O_3 coatings exhibited relatively dense columnar grained microstructure as compared with 8YSZ (Fig. 9a). HfO_2-27 wt%Y_2O_3 coatings were also deposited under the similar processing parameters (Fig. 7b). The coating exhibited an even relatively denser microstructure in comparison with the HfO_2-40 wt%ZrO_2-20 wt%Y_2O_3 (Fig. 9a). X-ray diffraction showed that both HfO_2-27 wt%Y_2O_3 and HfO_2-40 wt% ZrO_2-20 wt%Y_2O_3 have a cubic phase structure. Texturing of the cubic HfO_2-27 wt%Y_2O_3 coating growth changed as substrate temperature was increased from 1000 to 1100°C as evident in the X-ray diffraction pattern (Fig. 10).

The thermal conductivity of the HfO_2-40 wt%ZrO_2-20 wt%Y_2O_3 and HfO_2-27 wt%Y_2O_3 coatings were measured by the steady-state CO_2 laser technique. As shown in Fig. 11a, the thermal conductivity of HfO_2-27 wt%Y_2O_3 was found to be the lowest (1.1 W/mK). HfO_2-27 wt%Y_2O_3 exhibited relatively low conductivity rate increase at high temperature due to its good sintering resistance as compared with ZrO_2-8 wt%Y_2O_3. In order to further reduce the thermal conductivity of HfO_2-27 wt%Y_2O_3, the layering concept

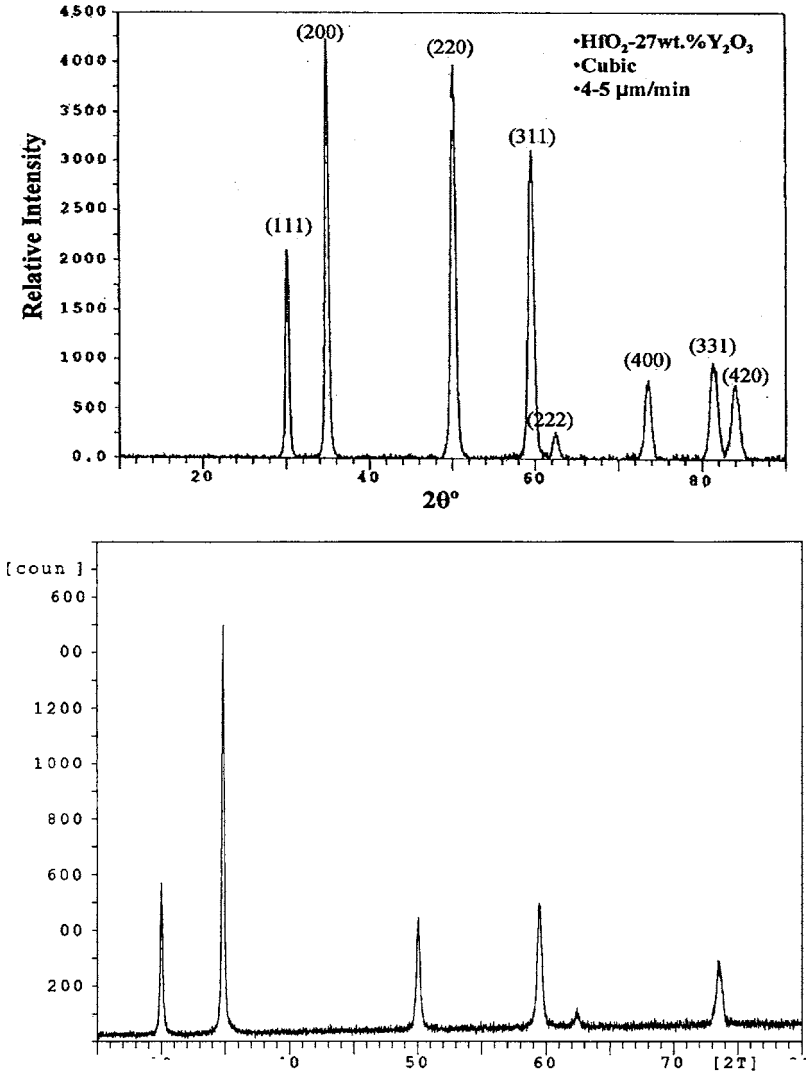

Figure 10 X-ray diffraction of HfO_2-27 wt%Y_2O_3 deposited by EB-PVD at 1000 and 1100°C, respectively, showing more texturing at higher deposition temperature.

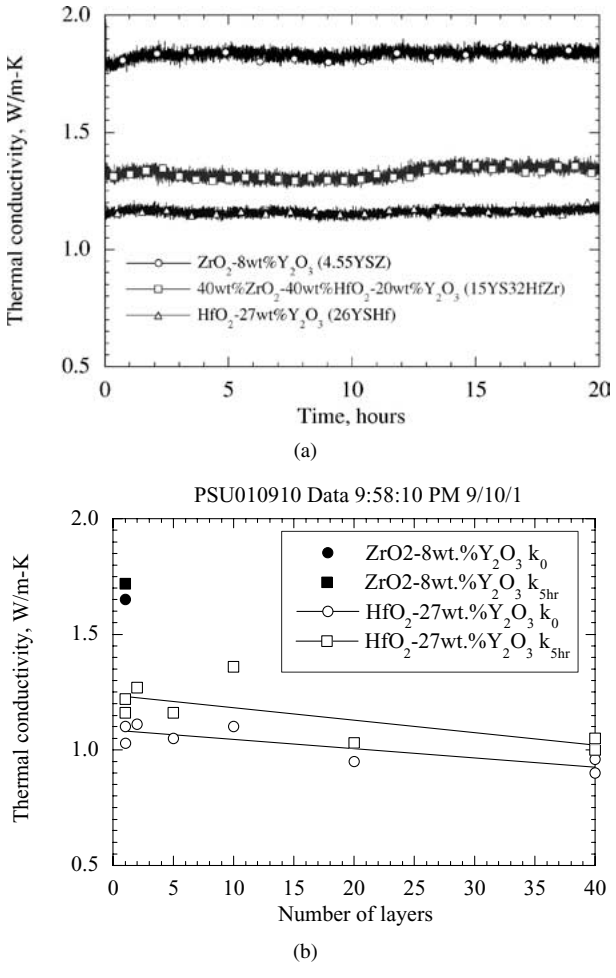

Figure 11 (a) Comparative thermal conductivity of EB-PVD 8YSZ, HfO_2-40 wt%ZrO_2-20 wt% Y_2O_3 and HfO_2-27 wt%Y_2O_3 coatings as a function of test time and (b) thermal conductivity of EB-PVD HfO_2-27 wt%Y_2O_3 coatings as a function of number of layers produced by "shutter" method.

was explored. The thermal conductivity of HfO_2-27 wt%Y_2O_3 was further reduced with increasing total number of layers (Fig. 11b). The thermal conductivity was measured in the same way as mentioned for Fig. 5b. Similar to the 8YSZ reflectance data, layering in the HfO_2-27 wt%Y_2O_3 coatings also exhibited an increase in hemispherical reflectance properties from 50 to 65% at 1 μm wavelength as shown in Fig. 12. These findings reconfirm previous findings in the 8YSZ, indicating that these are microstructural effects (and not compositional) which can be adapted to other TBC systems easily.

4. Summary

This research paper has demonstrated that tailoring the microstructure of TBC will allow engineering of potential new TBC materials with lower thermal conductivity and higher thermal reflectance properties. This concept can be extended to other TBC materials. Major achievements of the present findings are summarized below:

- Layered TBC structure exhibited reduction in thermal conductivity by 15–30% depending upon the volume fraction of micro-porosity.
- Layered TBC exhibited increase in reflectance by 12–15%.
- The HfO_2-27 wt%Y_2O_3 (HfO_2-25.6 mol%Y_2O_3) coating exhibited relatively low thermal conductivity, low rate of conductivity increase, and good sintering resistance as compare with ZrO_2-8 wt%Y_2O_3 and HfO_2-40% wtZrO_2-27 wt%Y_2O_3.

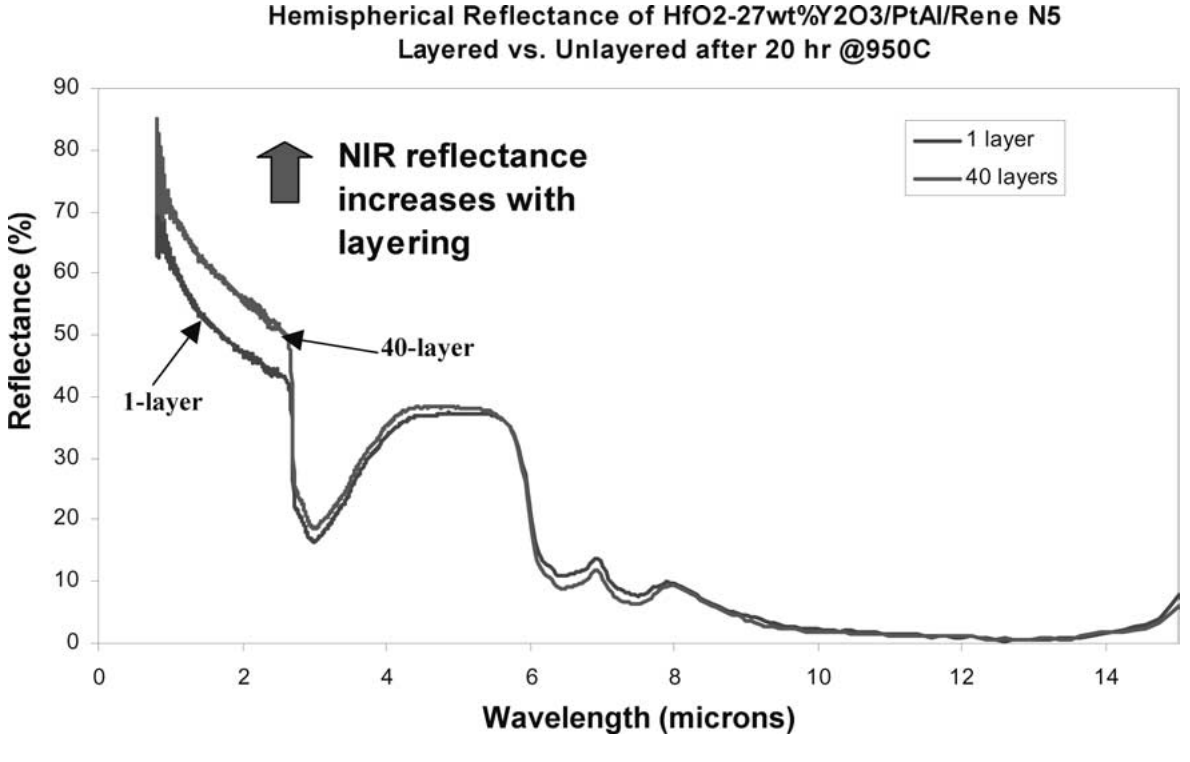

Figure 12 Hemi-spherical reflectance of HfO_2-27 wt%Y_2O_3 deposited on PtAl bond coated Rene N5 showing layered (shutter) vs. un-layered after 20 h @950°C.

Acknowledgement

This research was sponsored by the United States Navy Manufacturing Technology (ManTech) Program, Office of Naval Research, under Navy Contract N00039-97-0042. Any opinions, finding, conclusions, or recommendations expressed in this material are those of the authors and do not necessarily reflect the views of the U.S. Navy.

References

1. J. SINGH, D. E. WOLFE and JASON SINGH, *J. Mater. Sci.* **37** (2002) 3261.
2. H. HERMAN, *Sci. Amer.* **259** (1988) 112.
3. U. SCHULZ, K. FRITSCHER and M. PETERS, *Surf. Coat. Techn.* **82** (1996) 259.
4. U. SCHULZ, T. KRELL, U. LEUSHAKE and M. PETERS, "Graded Design of EB-PVD Thermal Barrier Coatings System," in Proceedings of AGARD Workshop on Thermal Barrier Coatings (Aalborg, DK, October 15–16, 1997).
5. D. ZHU and R. A. MILLER, *Ceram. Eng. Sci. Proc.* **23** (2002) 457.
6. J. I. ELDRIDGE, C. M. SPUCKLER, K. W. STREET and J. R. MARKHAM, *ibid.* **23** (2002) 417.

Received 29 May
and accepted 17 October 2003